Chemical Reviews

Volume 86, Number 3 June 1986

Diffraction Studies of Clusters Generated in Supersonic Flow

LAWRENCE S. BARTELL

Department of Chemistry, University of Michigan, Ann Arbor, Michigan 48109

Received September 27, 1985 (Revised Manuscript Received January 14, 1986)

Contents

Lawrence S. Bartell received a B.S. (1944) and Ph.D. (1951) from the University of Michigan where he has been a faculty member since 1965. Intervening periods were spent on the Manhattan Project, in the U.S. Navy, and on the faculty of Iowa State University. His research interests include structural chemistry and the dynamics of molecular processes.

I. Introduction

Clusters play crucial roles in fields ranging from atmospheric chemistry to industrial catalysis. An increasing awareness of their importance has stimulated the development of fresh methods for investigating their chemical and physical behavior. Although few would deny that a knowledge of their internal structure is indispensible to a satisfactory understanding of their properties, only a modest effort is being expended in direct structural research. An aspect of clusters that makes them particularly attractive objects for study also makes them troublesome to treat. Being larger than ordinary molecules but too small to be dealt with as bulk objects, they occupy a poorly understood niche that is ripe for exploration but not well suited for the traditional approaches of spectroscopy and X-ray diffraction. One tool in structural chemistry that offers promise in research on clusters generated in supersonic jets, the subject of this review, is electron diffraction.[1,2] Although new sources of intense, coherent X radiation are actively under consideration for the purpose,[3] electrons enjoy several strong advantages:

(1) They are scattered by small particles enormously more strongly than are X-rays or neutrons.

(2) They can be focused easily to yield a far higher resolution of diffraction detail than is customarily achieved in X-ray or neutron studies of weakly scattering objects.

(3) They are readily produced in intense beams capable of recording diffraction patterns with high signal-to-noise ratios in a fraction of a second.

0009-2665/86/0786-0491$06.50/0

(4) They can determine positions of hydrogen atoms far more definitively than can X-rays.

The present review will be limited, for the most part, to clusters generated in and studied during supersonic flow from miniature nozzles. Not covered will be important classes of clusters such as finely divided particles (e.g., platinum catalysts) dispersed upon solid supports. Usually the clusters examined by electron diffraction are much larger than those analyzed by spectroscopy and the character of the information sought is different. While clusters as small as a half-dozen molecules have been looked at with electrons, it is not uncommon to study clusters of thousands or tens of thousands of molecules. Questions of interest to workers in the field include

(1) What is the effect of cluster size on the internal structure and molecular motions?

(2) What can be learned about the dynamics of homogeneous nucleation and cluster growth?

(3) What can be learned about structures of liquids and amorphous solids in studies of supersonically generated clusters?

As we shall see, information of value in the resolution of all of these questions has been generated by electron diffraction. It has been found that atoms in small solid clusters do in fact pack together differently than in large clusters,[4-23] and the transition from one extreme to the other can be followed. Moreover, in the case of certain molecules, profound changes in the packing arrangement for a given cluster size can be induced by varying the conditions of nozzle flow,[24,25] and the structure can be probed microseconds after nucleation. Clusters may be liquidlike[26,27] or crystalline,[11-18] or mixtures of both.[26] For some substances liquidlike clusters can be studied at degrees of supercooling far exceeding those yet attained in the bulk.[27]

The special advantages of electron beams in signal-to-noise and resolution of diffraction detail have been realized in practice. This has opened up a promising avenue in the exploration of liquid structure where the full exploitation of electron diffraction has only become possible with the advent of the supersonic technique. Electrons are scattered too strongly to penetrate bulk liquid but are transmitted cleanly through, say, 100-Å clusters that are large enough to qualify as bulk phases as far as structure is concerned.

Electron diffraction is not the only experimental technique applied to draw inferences about the nature of clusters formed in nozzle flow. We briefly mention two other quite different approaches. By noting the presence or absence of "magic numbers" in mass spectra, Mühlbach et al.[28] had postulated that certain substances gave solid clusters, while others gave liquids. Another investigation[29] followed the gas dynamics in detail along a rather large nozzle during the condensation of water from moist, expanding air. A careful measurement of the profile of temperature and pressure was interpreted in the framework of classical nucleation theory. It was concluded that a liquidlike rather than an icelike surface tension was required for the critical condensation nuclei, but that the heat of condensation evolved from the growing clusters was that of solid water.

Clearly, the fundamental understanding of nucleation and cluster properties is a goal of such importance that it is worthwhile to apply a variety of experimental and theoretical approaches. As sketched above, electron diffraction is one of the approaches yielding encouraging results. To the best of this author's knowledge, only three laboratories have so far applied electron diffraction to cluster beams and each entered with a different purpose. The first of these, at Orsay, was expressly designed for clusters about 2 decades ago. Early work was largely carried out by Farges, Raoult, and Torchet, who together with de Feraudy, are still performing meticulous analyses of cluster structure and internal vibrations supplemented by molecular dynamics computations. The second laboratory was set up at Northwestern University in the early seventies by the late Gilbert Stein. Although his motivation was to test gas dynamics and nucleation theory, his researches carried him deeply into the characterization of structures and properties of clusters, as well. More recently, the present writer, long associated with electron scattering by gas molecules, entered the field with the notion that it might be possible to generate liquidlike clusters supersonically. Because the liquid state is to an overwhelming degree the least investigated structurally and the most poorly understood of the common phases, the venture seemed a worthwhile gamble. Results of the various approaches are presented in the following sections after a review of the experimental methods employed and the principles upon which they are based.

II. Experimental Methods

A. Electron Diffraction

1. Qualitative Review of Principles

Chemists are less familiar with diffraction studies of noncrystalline materials than with conventional spectroscopic and crystallographic techniques of structural chemistry. Therefore, it may be worthwhile to sketch the principles involved in order to convey what can be learned about clusters by electron diffraction. The essential ideas are very simple and can be understood in terms of the familiar *double-slit* interference experiment—because all diffraction features from cluster beams can be expressed in terms of contributions from *pairs* of sites that scatter electrons. If a wavefront encounters two fixed scattering sites, the waves are diffracted in all directions by each site. When scattered wavelets from the sites are combined at, say, a photographic plate (see Figure 1), they will be out of step with each other by an amount $(d_b - d_a)$ corresponding to the path length difference. As the scattering angle θ increases, this path difference also increases; it is $r_{ab} \sin \theta$ in the plane of Figure 1. Constructive (or destructive) interference occurs when the path difference is an integral (or half-integral) number of waves and the resultant interference fringes can be recorded and measured. Constructive interference fringes occur, then, at

$$r_{ab} \sin \theta_n = n\lambda \qquad (1)$$

where n is an integer. From the known wavelength λ and measured angles θ_n can be calculated the distance r_{ab} between scattering centers.

This elementary construction can be generalized to illustrate what happens when a monochromatic electron

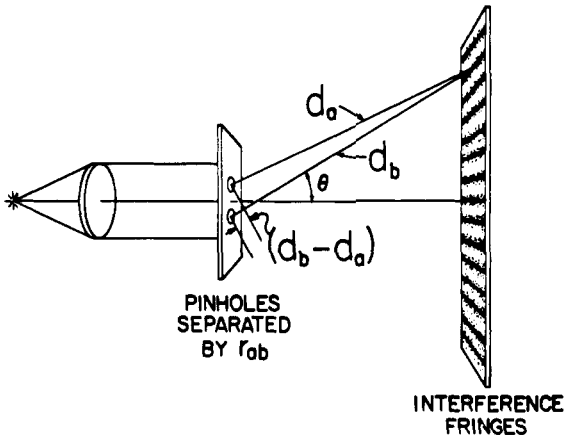

Figure 1. Illustration of interference fringes produced by waves diffracted from two scattering centers separated by r_{ab}. Constructive interference results when the path length difference $d_b - d_a = r_{ab} \sin \theta$ is an integral number of wavelengths.

beam ($\lambda = h/mv$) is scattered by a stream of randomly oriented clusters (or what is easier to visualize, a single cluster tumbling chaotically over all orientations). Consider, first, the set of fringes corresponding to any given pair of atoms in the cluster. The fringes would gyrate in synchrony with the tumbling. What is crucial is that a well-defined interference pattern survives this tumbling though, of course, in somewhat washed out form. Because no orientation is preferred, the pattern is circularly symmetric about the axis of the electron beam. It is not difficult to show that the interference intensity contributed by the atom pair ij consists of diffuse haloes whose intensity

$$I_{ij}/I_0 = f_i f_i (\sin sr_{ij})/sr_{ij} \qquad (2)$$

oscillates about the smooth background of atomic scattering. In eq 2 s is the scattering variable $(4\pi/\lambda) \sin \theta/2$ while f_i and f_j are widely tabulated scattering factors approximately proportional to the atomic numbers Z_i and Z_j. A little reflection confirms that the spacing between the haloes of eq 2 is comparable to the fringe spacing implied by eq 1, as it should be.

Because of the random orientation, all pairs of atoms play identical roles in scattering except for scale factors, and all contribute haloes characterized by eq 2. Widely spaced atoms give closely spaced haloes and covalently bonded atoms produce relatively widely spaced haloes. Again, internuclear separations can be inferred from the spacing. Diffraction features can only have a sharp appearance if they have components $\sin sr_{ij}$ that turn over in a short range of θ. Since such components can only arise from large internuclear separations, information on cluster size can be derived from the sharpness of diffraction features, especially the innermost diffraction rings. The fact that the net interference intensity is the sum of a great many sinusoidal contributions, each with a period directly related to an r_{ij} value, means that a harmonic (Fourier) analysis can be performed to determine what sine curves contribute to the intensity. This leads to a radial distribution function of internuclear distances in the cluster. In principle, a cluster with N atoms would exhibit $N(N-1)/2$ internuclear distances which, if well-resolved, would provide more than enough information to establish the $3N - 6$ atomic coordinates describing the structure. In practice, the peaks $P_{ij}(r)$ in the radial distribution function overlap too severely to allow a unique reconstruction of the detailed internal structure of a cluster. Examples of the patterns corresponding to various types of clusters and how cluster properties can be interpreted from them will be covered in a later section. First, let us put the foregoing ideas into a more quantitative language that will facilitate a description of the diffraction analyses.

2. Basic Relations

According to the foregoing discussion, small randomly oriented fragments of matter give diffraction patterns expressible in terms of probability distribution functions $P_{ij}(r)$ of individual atom pairs. This is true for free molecules, liquid clusters, and microcrystals as well, as developed in the following equations, starting with one for the net intensity

$$I_{net}(s) = K(I_{int} + I_a) \qquad (3)$$

where K is a factor depending on the concentration of scatterers and incident intensity, while I_{int} and I_a represent the contribution of a single molecule or cluster to the *interference terms* of interest and to the smooth *atomic scattering* that would occur regardless of the organization of atoms in the molecule or cluster. Atomic scattering[2,30]

$$I_a = \sum_i [|f_i(s)|^2 + t_i S_i(s)] \qquad (4)$$

is a simple sum over the atoms in the object, where $f_i(s)$ is the elastic scattering factor for the radiation being used, $S_i(s)$ is the inelastic scattering factor, and t_i is nearly unity for X-rays or $(2/a_0 s^2)^2$ for electrons with a_0 the Bohr radius. Tables of scattering factors exist for most atoms.[31-33] A straightforward extension of eq 2 gives

$$I_{int} = \sum_i \sum_{<j} 2 \text{ Re } f_i^* f_j \int_0^\infty P_{ij}(r) \frac{\sin sr}{sr} dr \qquad (5)$$

For heavy elements the electron scattering factors f_i are complex with a decided imaginary component but this complication is simple to handle and has been of negligible effect in clusters studied to date.

Note that I_{int} is the sum

$$I_{int} = I_{mol} + I_{Cl} \qquad (6)$$

of I_{mol}, the *intramolecular* interference terms and I_{Cl}, the cluster intermolecular interference terms. All of the structure information derivable about clusters, then, resides in the term I_{Cl}. It is convenient and common to express this term in the reduced form

$$M_{Cl}(s) = I_{Cl}/I_a^e \qquad (7)$$

usually called the "structure function", where I_a^e is the elastic part of I_a of eq 4. For clusters of a single type of atom, the atomic scattering factors cancel and the reduced function $M_{Cl}(s)$ is the same for electron, X-ray, or neutron radiation. For clusters of molecules containing more than one kind of atom the scattering factors no longer cancel and there may be differences, often modest, between structure functions derivable from different types of radiation.

In practice $M_{Cl}(s)$, the intermolecular function, can be derived from intensity measurements by subtracting

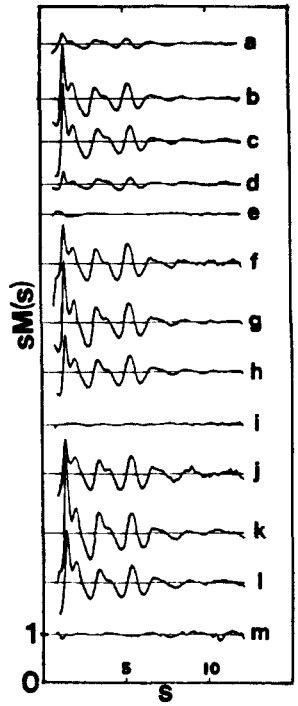

Figure 2. Experimental s-weighted structure functions for benzene clusters showing interference features characteristic of liquid structure. Helium carrier, curves a–e; neon carrier, curves f–i; argon carrier, curves j–m. In each case benzene mole fraction increases and carrier pressure falls. Reproduced, with permission, from Valente.[27] Copyright 1984, American Institute of Physics, New York.

from $[I_{int}/I_a^e - 1]$ the function I_{mol}/I_a^e. This molecular function can be derived either from experimental measurements on unclustered vapor molecules or from analytical calculations if the molecular structure is well-known.[34] Theoretically generated structure functions for comparison to experiment can be readily calculated from the foregoing equations if a histogram of the intermolecular distances is available from some theoretical model. Illustrations of what the structure function looks like for different types of clusters are given in the next section.

Before showing them, however, a few comments need to be made about notation. Unfortunately, the literature on structure functions is chaotic because workers in various areas have introduced a variety of different symbols. The quantity $(4\pi/\lambda) \sin(\theta/2)$ called s by the three cluster laboratories and adopted herein is not uncommonly called k or q in the field of liquid diffraction, and crystallographers are inclined to use the notation $(\sin\theta)/\lambda$, instead, and to mean by it $[\sin(\theta/2)]/\lambda$ because θ to them is the Bragg angle. Cluster publications from Orsay or Northwestern seldom refer to the structure function, often plotting s^3I_{net}, instead. In liquid diffraction the structure function is often represented by $H_d(k)$, $S(q)$, or $i(s)$.

3. Inferences of Cluster Properties

Examples of structure functions are shown in Figure 2 (in this case, multiplied by s) for benzene clusters produced under a variety of different expansion conditions.[27] That the diffraction haloes are more or less sinusoidal in aspect betrays a liquidlike structure. The initial diffraction feature, however, is fairly sharp, implying the presence of intermolecular distances of at least 30 Å and, hence, implying a cluster at least that

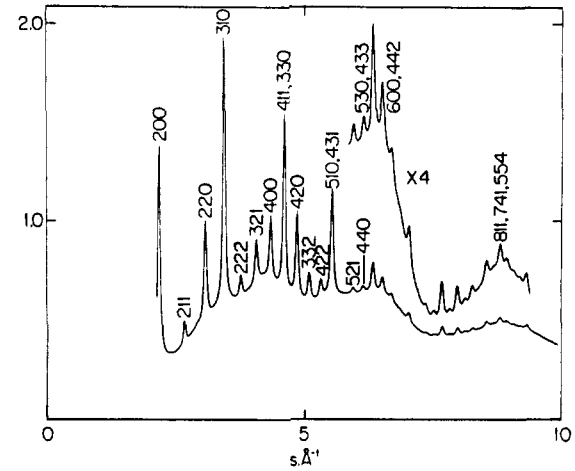

Figure 3. Experimental reduced intensity curve for crystalline clusters of SF_6 showing the relatively sharp Debye–Scherrer diffraction rings superposed on the broad molecular oscillations. Helium was the carrier gas. Reproduced, with permission, from Heenan et al.[35] Copyright 1983, American Institute of Physics, New York.

large. Crystalline clusters, on the other hand, give fairly sharp diffraction rings of the sort illustrated in Figure 3 for SF_6 clusters[35] (where the conspicuous molecular undulations have not yet been subtracted out). These rings can either be thought of as (slightly blurred) reflections from Bragg planes or as the superposition of sin sr_{ij} terms (of eq 2) with harmonic progressions of r_{ij} values. Such rings may be identifiable with the rings in the powder diffraction pattern of some known crystalline phase. Those in Figure 3, in fact, correspond to the plastic-crystalline body-centered cubic phase of SF_6.[24]

In the case of crystalline clusters it may be possible to deduce the temperature and cluster size quite directly. From the ring radii can be estimated the lattice constants. If, in addition, the lattice constants are known at a definite temperature from previous work and the coefficient of thermal expansion is known, the temperature can be deduced. For very small clusters a correction may be needed to take into account the compressive effect of surface free energy or the loose structure of surface layers (not all details are established).[36] An alternative measure of the temperature in some cases may be extracted from the rate at which intensities of diffraction rings, indexed hkl, fall off with scattering angle.[17,18,36,37] From the observed fall off, expressed as the Debye–Waller factor[36,37]

$$I_{hkl}^{obsd}/I_{hkl}^{calcd}\ (\text{rigid lattice}) = \exp(-\langle u^2\rangle s^2/3) \qquad (8)$$

can be inferred $\langle u^2\rangle$, the mean square amplitude of thermal motion of the scatterers. If the elastic constants of the lattice are known, $\langle u^2\rangle$ implies the temperature. For finer details, consult ref 36 and 37.

Sizes of crystalline clusters can be estimated from diffraction ring breadths, as can be understood at once from the uncertainty principle.[38] If an electron has been scattered by a cluster of diameter D, its uncertainty in lateral position is no more than $\Delta y = D$. Therefore it must have an indeterminacy in lateral momentum of order $\Delta p_y \approx h/D$ which will blur the diffraction rings by an amount the order of $\Delta s \approx 2\pi\Delta\theta/\lambda \approx 2\pi(\Delta p_y)/p)/\lambda \approx 2\pi/D$.

If a crystalline cluster is approximately spherical a more quantitative calculation shows that the top 95%

of each diffraction ring profile is very nearly Gaussian in shape with a fullwidth at half-maximum, in s units, of[39]

$$W = 6.953/D \quad (9)$$

It may be necessary to remove instrumental broadening effects from W_T, the total width, a useful approximation being

$$W \approx (W_T^2 - W_0^2)^{1/2} \quad (10)$$

where W_0 is the instrumental FWHM. More commonly is found the Scherrer formula[40]

$$W = 2\pi/D \quad (11)$$

derived for prisms of thickness D perpendicular to the Bragg plane reflecting the radiation (no crystal, of course, can be a right rectangular prism with external faces parallel to *every* Bragg plane). If clusters were polycrystalline or crystalline with imperfections, the ring breadth would be a measure of the size of individual well-ordered domains, not of the diameter of the cluster itself. In experiments to date, however, observed[41,42] D values from application of eq 9 are in approximate agreement with cluster diameters calculated according to classical nucleation theory,[42,43] and there is little reason to believe that individual growing nuclei collide and agglomerate.[44]

Diffraction patterns of liquidlike clusters provide less detailed information about structure, temperature, and density. Breadths of the internuclear distance peaks in the radial distribution function (pair correlation functions) still govern the rates of attenuation of intensities of diffraction haloes. Whether the breadths of the radial distribution peaks arise from dynamic motions of molecules in a liquid, say, or frozen disorder in a rigid amorphous solid cannot be deduced from the pattern of elastically scattered electrons, however. For small clusters of perhaps a dozen atoms it would be feasible to determine the detailed structure by electron diffraction just as one does in the case of gas molecules,[45] provided the cluster beams were separated into fractions of uniform mass. In practice, to date, such mass fractionation[41,46] has reduced cluster beam intensities to levels too low to give satisfactory diffraction patterns. The most fruitful approach to the analysis of noncrystalline clusters has been to compare observed structure functions with those calculated according to various proposed models or simulations based on statistical mechanics.

Distributions of sizes of clusters produced by a given procedure cannot ordinarily be determined from electron diffraction patterns. Mass spectrometry has been applied in some cases.[28,46,47] In others, clusters have been collected and examined by electron microscopy for size distribution.[42] The simplest but most speculative method is to simulate nucleation and growth using classical nucleation theory, and to compute the distribution. Even though there are some unsatisfactory aspects of the theory, calculated and observed mean sizes so far reported have been in reasonable agreement and in the one example reported, the calculated size distribution agreed quite well with that observed by electron microscopy.[42] Under common conditions of expansion, calculated distributions imply that the half-width at half maximum of the distribution depends upon conditions and may range from 10 to 40% of the most probable radius.[39,42]

4. Comments about Multiple Scattering

Despite potential advantages of electron beams in studies of matter, relatively little effort has been expended upon liquids. Prior attempts to obtain unambiguous, quantitatively interpretable diffraction patterns of electrons scattered by liquids have been impeded by multiple scattering and absorption. Scattering cross sections are very high. For example, for 40-kV electrons the elastic[48] and inelastic[49] cross sections for scattering from benzene molecules are 0.11 and 0.45 Å^2, respectively, and the density[50] of cold condensed C_6H_6 corresponds to about 1 molecule per 140 Å^3. Therefore, electrons will suffer more than one scattering, on average, when the length they must travel in condensed benzene is greater than about 250 Å [or 140 Å^3/(0.11 + 0.45) Å^2]. Considerations of this sort pertain to the *incoherent* multiple scattering by random arrays of molecules. (*Coherent* multiple scattering is discussed in the following paragraph.) Calculations[51] and measurements[52] of the incoherent effect show that diffraction patterns become washed out and more rapidly damped when electrons, on average, experience more than one scattering. It was found, however, that when interference features were attenuated by a factor of two through multiple scattering, the shapes and positions of the features were only modestly altered. Further attenuation led to excessive degradation of the pattern. Although a theory exists that can provide multiple scattering corrections if they are not large,[51] it is clear that electron diffraction patterns of high quality cannot be obtained for condensed phases unless some means is found to produce exceedingly thin samples. Nozzle flow generates satisfactory samples very naturally. An alternative procedure of considerable ingenuity but great technical difficulty and uncertain characterization was devised by Kalman.[53] In Kalman's technique a film of water brushed onto a special holder was thinned by evaporation until it would transmit electrons for an instant before being obliterated.

The above discussion pertains to multiple scattering with random phase relations between scatterings. When electrons are diffracted by a well-defined scatterer such as a periodic lattice or a fairly rigid molecule, another type of multiple scattering, "dynamic scattering," coherent in nature, arises. It can exacerbate the situation because elastic amplitudes rather than intensities are added. Questions have been raised about work with crystalline clusters because dynamic scattering effects can even be seen to complicate the patterns of electrons scattered by *single molecules*![54] By contrast, dynamic scattering is seen in X-ray or neutron diffraction only when samples reach macroscopic thickness. Theories of dynamic scattering exist both from the standpoint of building up scattering systems atom by atom[54,55] and of subdividing crystals to smaller and smaller units.[20] For small clusters of organic molecules corrections can be ignored.[56] For large clusters of metals it is wise to apply them. Gold clusters only 16 Å in diameter gave calculated dynamic effects in intensities exceeding 25%. Only for large diameters, however, were the intensities of the rings *relative to each other*, greatly distorted.[20]

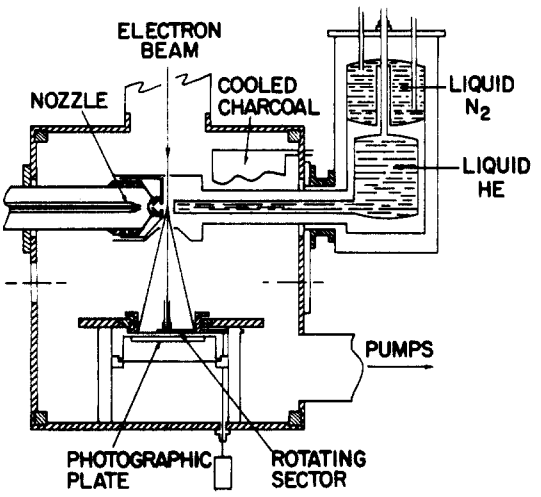

Figure 4. Schematic diagram of the diffraction chamber of the Orsay apparatus. Gas expands from the miniature nozzle at the left into the skimmer chamber evacuated by a Roots pump. Gas transmitted through the skimmer and collimator is probed by an electron beam before being condensed on surfaces cooled by liquid helium. Scattered electrons are filtered by a rotating sector, then recorded on a photographic plate. Redrawn from Raoult and Farges.[57]

5. Diffraction Apparatus

Illustrated schematically in Figure 4 is the Orsay electron diffraction unit.[57] A conventional electron optical system produces a fine beam intersecting the effluent from the nozzle-skimmer assembly. Electrons scattered by the cluster beam are recorded on a photographic plate taking several precautions to ensure records of high quality. The electron beam is focussed by a magnetic lens above the nozzle to direct all electrons scattered through a given angle sharply to a common radius of the plate. A rotating sector is interposed between the point of scattering and the plate to act as a filter and restrict recorded electron flux densities to a fairly narrow range. Without the rotating sector, electron intensities would vary over the photographic plate by several orders of magnitude, prohibiting accurate photographic measurements of pattern intensity. Because diffraction patterns are circularly symmetric, the diffraction plates can be rotated during photometry to average over grains in the emulsion. In careful work, sensitivity to diffraction detail more delicate than 1 part per thousand of the background atomic intensity can be obtained.[45] Cryopumping at liquid helium temperatures augments a diffusion pump in scavenging gas from the diffraction chamber.

The Michigan unit,[35,45] originally designed for different purposes, is qualitatively similar to its Orsay counterpart but adopts a simpler nozzle system, uses liquid nitrogen instead of helium, compensating, in part, by incorporating pumping lines of large diameter. The most recent version of the Northwestern unit introduced an electron counting system to replace film recording in an attempt to improve precision in the measured diffraction patterns.[58] The resultant digitally recorded patterns, however, have yet to approach the signal-to-noise ratios achieved in standard sector microphotometer measurements made upon high quality photographic plates when provision is made to integrate over plate areas exposed to $\sim 10^8$ electrons and to integrate over a precisely integral number of revolutions of the plate.

One feature greatly facilitating accurate observations of the innermost diffraction details was the fabrication of a miniature rotating sector[27] with a useful range inside $s = 1$ Å^{-1}. Construction followed Kalman's simple but effective design[53] for small angles of joining two circular disks and rotating the pair about the point of contact. An improved compensation for the rapidly falling electron intensity was obtained by milling flat a short portion of the edge of each disk before joining the disks along the flat segments.

B. Supersonic Nozzle System

The Orsay system is based on Campargue's design[59] of a supersonic configuration to achieve high throughput with modest pumps while preventing invasion of the jet by background gas. Gas at pressures from perhaps 100 torr to tens of atmospheres expands from a small tubular nozzle toward a skimmer. Most of the gas is skimmed off at a pressure of the order of 1–500 millitorr and exhausted from the expansion chamber by a Roots pump. Gas transmitted through the skimmer is skimmed again by a collimator 15 mm downstream, after which the collimated jet is probed by the electron beam. This system has many advantages, including a ready capability of generating clusters from neat gases, and a simple means of determining the position of shock waves. Clusters can be studied unshocked or, if desired, annealed by passage through a shock wave. Most investigations at Orsay have been carried out with neat gases.

The Northwestern system is similar,[58,60] including the skimmer and collimator. A miniature glass Laval nozzle,[61] however, replaces the tubular nozzle. Supersonic flow is attained within the nozzle itself, and nucleation and cluster growth are completed (or nearly so) before gas exits the nozzle. This contrasts with the Orsay system where nucleation and growth take place during the free jet expansion between the nozzle and collimator. Another difference is that, in the Northwestern system, a carrier gas, usually He, Ne, or Ar, accompanies the material to be condensed through the nozzle and plays an important role in governing the kinetics of the cluster formation. It controls flow speed, helium transporting the seed gas much faster than, say, does argon, and it carries off heat of condensation, argon more efficiently than helium.

The Michigan nozzle system[35] is more primitive than the others. It resembles the Northwestern system in its incorporation of a Laval nozzle and skimmer but dispenses with the collimator. A carrier gas is usually used, as well. The shock wave structure is as yet unmapped. The main virtue of the system is its simplicity and compatibility with a diffraction unit designed for other purposes. Despite its severe simplicity and recent entrance into cluster research, the nozzle has produced the greatest variety of cluster types so far seen by any system.

Several characteristics of a Laval-type of nozzle make it useful for cluster studies.[61] By definition, it is a nozzle that flares out beyond its throat (position of minimum cross section area). Only with such a nozzle will supersonic flow and the attendent temperature drop be achieved inside the nozzle itself. The nozzle walls impose a severe constraint on the rate of expansion, thereby considerably slowing down the temperature

drop and greatly increasing the number of collisions between molecules in comparison with a free jet expansion over the same temperature drop. Laval nozzles, therefore, are more efficient generators of clusters and can give satisfactory results with much milder flow conditions and smaller pumping requirements.

III. Statistical Modeling of Clusters

Three statistical techniques commonly applied to the structure and thermodynamic properties of condensed phases are identified here to avoid distracting elaborations in later sections. Especially when noncrystalline clusters have been encountered it has proven to be helpful to interpret diffraction patterns in terms of one or more of the following statistical approaches, molecular dynamics, Monte Carlo calculations, and the reference-interaction-site model (RISM). All of the methods depend upon an explicit representation of the potential energy surface characterizing the ensemble of molecules to be treated. Partly for reasons of economy and partly out of ignorance of many-body force laws, atom–atom pairwise additive interaction energies are almost always adopted. Lennard–Jones (6–12) potential functions have been the most popular partly, again, because they are cheaper to calculate than Buckingham and more complex functions that are superior representations of observed interactions and, partly, because a rich background of information on Lennard–Jones systems is already available to provide guideposts, even if the systems are artificial. In the case of polyatomic molecules, in particular, optimum potential energy functions have not yet been established. Nevertheless statistical modeling is yielding rich insights about condensed matter. The three techniques encountered in the review of results are sketched below only in barest outline to distinguish them from each other. For further details review articles should be consulted.[62-65,68-70]

A. Molecular Dynamics

In the method of "molecular dynamics" (MD)[62-64] the trajectories of individual members of a small collection of molecules are calculated as the molecules undergo chaotic collisions. Commonly the systems comprise a few dozen to a few hundred molecules, though as many as several thousand have been included.[67] These may be placed in a cluster possessing a surface or in a cell with periodic boundary conditions to simulate bulk matter with only a small assemblage of individuals. Molecules interact through some assumed potential energy function and move according to Newtonian mechanics. Their mean kinetic energy is a direct gauge of the temperature, and runs can be made with full control over temperature and pressure or density. From such runs can be computed pair correlation functions for various atoms, groups of atoms, or centers of mass, the equation of state, and standard thermodynamic functions. In addition, certain kinetic quantities such as self-diffusion coefficients and transport properties can be inferred.

B. Monte Carlo Calculations

Monte Carlo (MC) computations[64-66] are similar to MD simulations in the size and types of molecular systems studied. Instead of generating a thermal distribution by random collisions, however, random molecules are moved through random displacements by some prescription, and the move is accepted or rejected according to the Metropolis criterion. After a great many moves ($\approx 10^6$) the system is in a Boltzmann distribution at a controllable temperature and pressure or density. While MC runs do not give as intimate a view of molecular processes as MD runs, they yield comparable pair correlation functions and thermodynamic information, and can characterize transport properties, as well,[64] though in the hands of chemists they have mainly been applied to equilibrium properties.

C. Reference-Interaction-Site Model

The reference-interaction-site model (RISM) has evolved from the approximate solution of the integral equations of fluids in statistical mechanics via consideration of the direct correlation function of Ornstein and Zernike.[68] The Percus–Yevick approximation provides a closure relation for the Ornstein–Zernike equation and renders numerical solutions of pair correlation functions tractable.[69] Originally the method was applied to monatomic hard-sphere liquids, then generalized by Lowden and Chandler[70] to polyatomic molecules in which component atoms were treated as hard spheres. Finally, it was extended by Johnson and Hazoumé[71] to treat more general interaction functions. The principal advantage of RISM over MC and MD calculations is that it is considerably less expensive to apply, and it is supposed to be excellent if densities are not too high. Its accuracy in handling actual liquid systems has been analyzed only comparatively recently. Although MC and MD can be applied explicitly to small clusters, solid or liquid, in principle, RISM is intended to handle bulk liquids.

IV. Results

A. Clusters of Monatomic Molecules

Rare gases and, to a lesser extent, metals, have been the most popular subjects of diffraction investigations of clusters to date. This is quite natural for several reasons, not the least of which is that chemists have only recently invaded this field previously enjoyed solely by physicists and gas dynamicists. Monatomic systems offer advantages. Not only are their dynamics of expansion and condensation more elementary to treat theoretically than those of polyatomic systems but also the diffraction patterns they yield are simpler to decipher. All of the diffraction detail visible over and above the smooth background of atomic scattering is immediately ascribable to the cluster structure. No corrections for intramolecular interference terms need be made and no orientational factors complicate packing arrangements.

Though simple, these systems have yielded fundamental insights about the structure and dynamics of matter intermediate in spatial extent between molecules and bulk. The influence of fineness of subdivision of matter isn't merely a matter of a distinctive surface layer of molecules becoming more conspicuous when the proportion of surface molecules increases. Rare gas and at least some metal atoms choose to pack together differently in small clusters than in large ones. How

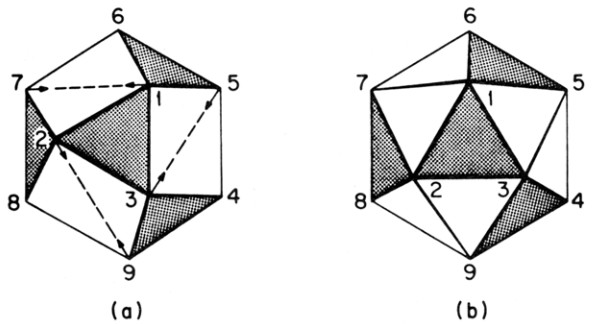

Figure 5. Transformation (arrows) from a cuboctahedron (a) into an icosahedron (b). Redrawn from Farges et al.[14]

this influences the kinetics of nucleation and catalysis is an open question of great significance. A brief outline of the effect of cluster size upon cluster structure is as follows.

At temperatures below their freezing points, large clusters of rare gas atoms and certain metals (e.g., Pb and Ag)[20] crystallize into cubic closest packed arrays (fcc lattices). While this is the most efficient space-filling form for spheres in the bulk (insofar as anyone knows) it is *not* the most stable arrangement for small numbers of soft, mutually attracting spheres. This conclusion was suggested by computations of packing energies of Lennard–Jones spheres by Hoare and Pal[4-6] whose results were in harmony with the earliest experimental observations of small argon clusters by the Orsay group. To give an example, the most stable packing of 12 rare gas atoms around a central atom is a regular icosahedron visualizable as made up of 20 identical (but slightly distorted) tetrahedra sharing a common vertex (the central atom). The corresponding 13-atom fragment of cubic closest packing is a cuboctahedron with 6 atoms surrounding the central atom in an equatorial plane, three more atoms sitting in indentations above the plane, and three, below. Identical tetrahedra, this time regular, can be identified in the cuboctahedron, also, but there are altogether only 8, not 20.

Mackay showed in 1962 how simple deformations from one form could lead to the other.[72] Figure 5 illustrates the transformation for 13-atom cluster. Detailed discussions by Mackay,[72] Hoare and Pal,[4-6] and the Orsay group[11-18,73] treat smaller clusters, and larger ones, as well, considering further growth upon the faces of the icosahedral unit that preserve an underlying icosahedral signature. As is well known to students of crystallography, there is no space group admitting such packing and, hence, no true crystals can be built up by growth upon icosahedra. Successive layers added to the icosahedral faces lead to increasing strains. Even the 13-atom fragment is not strain-free. The radial atom–atom distances are compressed to lengths 5% shorter than the outer, tangential distances. Beyond a certain size, multilayer icosahedral structures become less stable than fcc. Experimental diffraction patterns of rare gas clusters closely parallel those based on theoretical simulations by molecular dynamics. At temperatures of formation characteristic of the Orsay nozzle system (see below) clusters progress from amorphous ("polyicosahedral") for $\bar{N} < 50$ atoms/cluster through multilayer icosahedral for $50 < \bar{N} < 800$ to fcc when $\bar{N}$ exceeds about 800 atoms/cluster.[13,17,74] There is some indication[21-23,75] that for colder clusters, grown in the presence of an expanding carrier gas, the transition to fcc is delayed until the mean size reaches a few thousand atoms. Although the smaller clusters with polyicosahedral or multilayer icosahedral structures are noncrystalline, they are solid. For clusters larger than $\bar{N} \approx 100$ atoms their diffraction patterns are sharper than characteristic liquid patterns. Moreover, MD runs betray no liquidlike self-diffusion, and unmistakable melting occurs in MD simulations as the temperature is increased to the melting point.[17]

Icosahedral packing recently received widespread attention[76,77] due to the convergence of two observations, one experimental,[78] and one theoretical.[79,80] It was discovered[78] that certain rapidly quenched alloys sometimes yield metastable quasicrystals displaying sharp, well-ordered diffraction spots manifesting 5-fold symmetry. Sizes of these quasicrystals may exceed 1 μm, with Bragg planes appearing to be well aligned across the entire ordered domain. Independent mathematical modeling[79,80] showed how space-filling subunits ("Penrose patterns") with an icosahedral motif can be put together to produce a quasi-periodic structure. When the Fourier transform was computed, it implied a diffraction pattern that turned out to be strikingly similar to the observed diffraction patterns of the alloys. While this is a provocative clue, the true internal structure of the quasicrystals remains incompletely understood.

Although metal clusters have been studied intensively by several techniques, they have received much less attention than rare gases in diffraction investigations. When they have been investigated,[19,20,37,81] conditions of the vaporization and nozzle flow have been decidedly different from those of the rare gases, and the measurements of diffraction intensities, more rough and ready. Nevertheless, the diffraction patterns of metals that normally crystallize in the fcc habit in the bulk (Pb,[37] Ag[20]) closely resembled patterns of rare gas clusters of comparable size. In particular, they exhibited the same characteristic deviation from the fcc patterns now associated with correlations in atomic motions in small crystals deviating from those in the bulk.[82]

One remarkable investigation of nucleation in supersonic expansion deserves mention even though the clusters formed were not subjected to structure analyses. Sherman et al.[42,83,84] produced metal clusters, principally Zn, in flows (through Laval nozzles with helium carrier gas) that were conceptually identical with the later expansions of volatile gases at the Northwestern and Michigan cluster laboratories. What stands in sharp contrast, however, is that the metal heats of vaporization and surface tensions were an order of magnitude higher, requiring temperatures to be scaled up, accordingly. Stagnation temperatures were brutal, sometimes exceeding 5000 K with pressures of 5000 psia, and nozzles eroded quickly. Because the clusters, once formed, were nonvolatile, they could be collected and examined for size and shape by electron microscopy. Clusters were in the 100-Å range, as they commonly are, also, in the analogous studies of volatile substances. The results of Sherman et al. are particularly valuable in demonstrating the influence of carrier gases and nozzle design and in permitting a quantitative comparison with classical nucleation theory. Despite

the formidable experimental difficulties, observed nucleation rates and cluster size distribution were well-modeled by the classical theory.

Temperatures of clusters as they exit the nozzle can be inferred from diffraction measurements of lattice constants and mean-square amplitudes of atomic motions, as outlined in a previous section.[36,37] Although cluster temperatures depend strongly on the substance condensed and upon the expansion conditions, the Orsay group found a very simple relationship applicable to their system.[74] Temperatures of clusters generated by the flow of neat gases through the Campargue nozzle were almost independent of initial (stagnation) pressures and temperatures. Moreover, how hot the clusters were depended little upon cluster size or internal structure, for a given substance. It was discovered that cluster temperatures were, to a good approximation, proportional to the well-depth of the interatomic potential energy. We here convert to heat of sublimation and rewrite the Orsay relation as

$$T_{Cl} \approx \Delta H_{sub}/B \qquad (12)$$

where B is a constant[85] with the value 0.20 kJ mol^{-1} K^{-1}. That B is dimensionally an entropy with a value twice the Trouton constant is interesting but of obscure significance. Alternatively, as suggested by the form of eq 12, the measured cluster temperatures are those for which the bulk sublimation pressure is very nearly 10^{-6} atm. Clusters of O_2, N_2, and CO_2 fell on the same curve as the rare gases. Illustrative examples of cluster temperatures are $T_{Cl}(Xe) = 79 \pm 8$ K, and $T_{Cl}(Ar) = 37 \pm 5$ K. Greater degrees of chilling can be achieved in expansions through Laval nozzles with carrier gases.

Mean cluster sizes are readily controllable from a few atoms per cluster to over 20,000, by adjusting initial temperature, pressure, and concentration of carrier gas. In experiments by the Orsay group with neat argon,[57,86] changes in pressure, alone, from a few hundred Torr to a few atmospheres changed the effluent from unclustered gas to large clusters. Conditions that lead to extremely small clusters are not conducive to the condensation of more than a small fraction of the gas. Diffraction patterns of such clusters are feeble, then, and difficult to measure with precision. On the other hand, conditions favorable for large clusters lead to condensation of most of the gas transmitted through the skimmer, and strong cluster patterns can be recorded, even in the presence of large excesses of carrier gas.

Additional structural research on clusters of monatomic substances is described in references 87–90.

B. Solid Clusters of Polyatomic Molecules

1. CH_4 and N_2

Methane and nitrogen are quasispherical molecules whose condensed phases have physical properties bearing some resemblance to those of argon. It is not surprising, then, to find that clusters of CH_4 and N_2 produced by the Orsay system behaved strikingly like those of Ar.[18] Small clusters with a few dozens of molecules exhibited polyicosahedral structures while clusters of several thousands of molecules were crystalline with molecular centers at fcc lattice sites. In the case of CH_4, whose central carbon atom dominates the scattering, the structure functions are virtually identical in appearance with those of argon clusters. Indeed, even methane's root-mean-square amplitudes of oscillation $\langle u^2 \rangle^{1/2}$ of 0.31 Å (or 5.2% of the cluster lattice constant) were close to the corresponding quantities 0.26 Å (or 4.8%) for argon clusters. Patterns of nitrogen molecules, whose scattering sites are displaced from the molecular centers, differed appreciably in appearance. Moreover, root-mean-square amplitudes were substantially larger at 0.51 Å (or 9.0%), no doubt, partly because of the contribution of librational motions of the molecules.

2. CO_2

Even though CO_2 is decidedly less spherical than the other molecules so far considered, its large clusters are similar in internal organization.[36] Carbon dioxide molecules pack in a cubic structure ($Pa3$) with carbons at fcc sites. Large clusters with diameters of several hundred angstrom units gave quite sharp Debye–Scherrer rings and root-mean-square amplitudes of 0.252 Å (for planes containing only O atoms) and 0.240 Å (for planes containing both C and O atoms). For smaller clusters, formed at lower gas pressures, the amplitudes as well as the difference between the O and C/O amplitudes steadily increased as the cluster diameter decreased, and the lattice constant shrank by about 1% as clusters reached 25 Å. The larger amplitudes of the smaller clusters reinforced previous experience with the Orsay condensation process (cf. eq 12) that the shrinkage of the lattice was *not* due to cooling. It could, however, be accounted for by the Laplace internal pressure, $4\gamma/D$, which of course is exerted more intensely, the smaller the cluster diameter. A plausible surface stress, γ, of 80 ergs/cm^2 suffices for the observed shrinkage. The increasing proportion of the looser surface molecules as the clusters become smaller explains the trend in mean-square amplitudes, and librational motions naturally make the O displacements larger than those of C atoms. Librational amplitudes were inferred to be 5° or 6° in the intermediate clusters, only slightly larger than those in the bulk.

Torchet et al.[36] interpret their diffraction patterns in terms of fcc packing at all cluster sizes down to the smallest they encountered, thereby drawing a distinction between CO_2 and Ar, CH_4, and N_2 which exhibit icosahedral packing for small N. This may in part be a matter of experimental sensitivity. Van de Waal,[91] in packing calculations on very small CO_2 clusters ($N \leq 13$ molecules) found that polytetrahedral or icosahedral structures closely analogous to those discussed above for Ar were more stable than fcc fragments.

3. H_2O

Clusters of water are decidedly different from the other clusters so far discussed.[92,93] Those studied to date, both at Orsay and Northwestern, were produced without carrier gas. In order to get vapor pressures in the required range, initial nozzle temperatures were elevated. Clusters ranging from several dozen to several thousands of molecules were obtained with stagnation pressures ranging from 1 to 7 atm. Large clusters were mainly crystalline, but of the diamond cubic phase, not of simple ice. Small clusters were amorphous, although they were believed to be solid, also. Temperatures of

all clusters generated at Orsay[92] were estimated to be about 180 K, partly on the basis of eq 12 and partly from comparisons between diffraction patterns and model calculations. Stein and Armstrong[93] assumed their clusters were colder than 150 K, the temperature of transition to the diamond cubic form.[94] A variety of popular models of water clusters were tested and found inadequate to account for the diffraction patterns of small clusters. These included models of dense random packing of tetrahedrally coordinated molecules[95,96] and several clathrate models.[97,98] A model which did give agreement was constructed by carrying out a molecular dynamics simulation with 20 H_2O molecules interacting through the Stillinger–Rahman potential function.[99] A droplet, initially liquid, was cooled to temperatures far below 0 °C in the simulation, giving a disordered hydrogen-bonded network with distorted rings of 3–6 H_2O molecules.

In one interesting set of experiments upon the larger clusters, skimmer conditions were altered to force the clusters to pass through a shockwave, thereby subjecting them to a brief heating.[92,100] This had the effect of annealing the microcrystals and increasing the degree of crystallinity. Similar experiments with CO_2, which had given well-ordered clusters at all conditions, showed no increase of ordering induced by the shockwave. Instead, the shockwave appeared to evaporate some of the surface CO_2 molecules.

4. SF_6, SeF_6, TeF_6, and Other Fluorides

Sulfur hexafluoride has been the most extensively studied molecule with the possible exception of Argon, having received attention from all three cluster laboratories.[24,25,35,41,43,61,101–104] It was a particularly convenient subject for a series of fruitful studies, experimental and theoretical, on gasdynamics and the kinetics of nucleation and cluster growth by Stein et al.[43,61] While these investigations were valuable and interesting in their own right, their detailed content is beyond the scope of the present review. The different procedures of the different laboratories led to contrasting results providing clues (not yet fully understood) about the mechanism and dynamics of nucleation.

The Orsay system, applying high initial pressures (20–40 atm) and nozzle temperatures cooled to 220 K, was able to produce SF_6 clusters ranging from 40 Å diameter, temperature 113 K (neat gas) down to 30 Å, 70 K (mole fraction 0.01 SF_6 in Ne).[104] Intermediate temperatures could be produced by passing the cold clusters through shockwaves. All clusters gave diffraction patterns corresponding to the plastic–crystalline bcc phase I believed to be stable in the bulk from its melting point (225.5 K at 2.2 atm) down to 94.3 K where it undergoes a transition to phase II whose character is not fully understood.[105–107] That the bcc phase was observed at a temperature 25 °C colder than the transition temperature is of some interest (see below) but is not surprising in view of the cluster's brief lifetime of tens of microseconds, only part of which was spent in a supercooled state.

Larger clusters (50 Å to over 170 Å) were easily achieved under much less severe conditions in Laval nozzles with carrier gases. Laval nozzles, as explained before, are more efficient generators of clusters. Stein et al.[41] reported bcc clusters of SF_6 (X_{SF_6} = 0.03 in Ar) with temperatures apparently decreasing to 70 K as stagnation pressures increased to 3.5 atm (nozzle temperature 293 K). While this does not look out of line with the Orsay data, it is not consistent with data on SF_6 and SeF_6 acquired later in similar Laval expansions at Michigan.[24,25] Moreover, Stein reported anomalous behavior of the apparent cluster size as a function of mole fraction and stagnation pressure. What has been observed in Ann Arbor for SF_6 and SeF_6 is the growth of intensity of a diffraction pattern of crystalline phase II that "contaminates" the phase I pattern as conditions become severe enough to drop nucleation temperatures below the transition temperature. Since diffraction rings of phase II appear close to those of the strong rings of phase I, they distort the pattern in a way that can lead to misinterpretation of cluster size and temperature if the "contamination" is not taken into account.

Strong lines of phase II were obtained more readily for clusters of SeF_6 than for SF_6,[24] presumably because its transition temperature (170 K)[108] is higher. Tellurium hexafluoride, with yet a higher transition temperature (233 K),[108] formed clusters of phase II with such ease that patterns of the bcc phase I were never seen.[24,25] In fact, on decreasing the temperature of nucleation, TeF_6 clusters of yet a third crystalline phase (so far unidentified) were produced. This could be brought about either by decreasing the TeF_6 mole fraction or decreasing the stagnation pressure. Phase II appears to be triclinic[25,106] although some reports suggest that the transition of SF_6 at 94 K is from bcc to hexagonal.[105]

Details of the crystallography of the hexafluorides and of the simulations under way to help resolve the matter are outside the subject of this review. What *is* significant is the control one has over the type of cluster that can be formed and whether, if low temperatures are attained, one has a supercooled or an equilibrium form. For example, for the hexafluorides at depressed temperature, cold form I or forms II or III can be grown, or a mixture of forms. How a mixture can appear is uncertain. One possibility is that first I, then II forms by homogeneous nucleation as the nucleation temperature drops through the transition point, before nucleation is shut off via the heat of condensation evolved by the growing clusters.

Other fluorides that have been observed to give crystalline clusters include SiF_4 and C_4F_8.[109] Flow conditions and cluster sizes are similar to those of the hexafluorides.

One behavior, first noted by Stein,[103] is that when SF_6 clusters are grown in expansions with Ar carrier at low concentrations of SF_6, Ar clusters can appear, too, under flow conditions similar to the production of Ar clusters from neat Ar. Such behavior has also been observed with a number of other seed gases at low concentration ($X < 0.03$) in Ar.[24,25] It was initially interpreted as the heterogeneous nucleation of Ar upon the surface of SF_6 clusters.[103] This seems doubtful because the Ar clusters are much colder than the SF_6[24] (and other) clusters, and the thermal conductivities could not allow such a gradient.[39] Indeed, the molecular clusters appear to be too warm to condense Ar under the flow conditions achieved, and it is probable that Ar fractionates away from the warm cluster jet concentrated on the central lines of flow and undergoes homogeneous nucleation as

it would in the absence of the seed gas.

C. Liquidlike Clusters of Polyatomic Molecules

1. General Remarks

Before chemists entered the field, all supersonically generated clusters studied by electron diffraction had been reported to be solid. Their constituent molecules had all been very simple, and most were spherical or quasispherical. As soon as chemists tried seeding carriers with more complex molecules, for example, various hydrocarbons, it turned out that a large proportion of them gave cluster patterns of very different aspect. Clusters were liquidlike. A full elucidation is not yet at hand but much useful evidence has accumulated.

2. CCl_4

Carbon tetrachloride was among the early substances observed to condense into liquid clusters.[26] It is noteworthy for several reasons. First, it is the only substance so far to have been induced to condense into either liquid clusters or crystalline clusters, depending upon conditions. Secondly, the distance over which order is seen in the liquid is quite large. Liquid clusters are obtained in expansion with carrier gas through a Laval nozzle when conditions are mild. As expansion pressures increase, diffraction features begin to transform into a superposition of rings corresponding to the rhombohedral plastic–crystalline phase. It is not yet possible to determine the temperature of the liquid clusters with accuracy but an estimate based on the temperature-dependent position of the innermost diffraction line suggests ~200 K whereas eq 12, found by the Orsay group to apply to some polyatomic cases, suggests a temperature below 150 K. In any event, the clusters appear to be substantially supercooled below the melting point of 250 K. Because the clusters are probably above the glass temperature estimated to be 129 K[110] and transform easily into crystals,[26] they are almost certainly liquid in nature, not amorphous solids. They also appear to be colder than the crystalline clusters whose densities correspond approximately to 225 K. Freezing of isolated supercooled liquid CCl_4 would raise the temperature by about 20 °C through evolution of the heat of fusion.

What stimulated research on CCl_4 in the first place were comments in the literature[111] that standard X-ray and neutron diffraction techniques give too poor resolving power of diffraction detail to show the true narrowness of profile of the innermost diffraction rings—and, hence, the standard technique far underestimates the true range over which the liquid exhibits order. A new energy-dispersive X-ray technique was introduced that was claimed to detect order out to 30 Å in liquid CCl_4.[111] Such a long range seemed remarkable for a molecule like CCl_4. Because it was not clear to what extent the novel X-ray technique could be trusted and because an electron beam can provide very high resolution, it was decided to carry out an electron study of CCl_4 clusters. The result was even more remarkable than that of the energy-dispersive X-ray examination. Order was found beyond 50 Å for the microdrops of supercooled liquid!

One statistical model has been applied to both liquid[112] and glassy[113] (10 K) CCl_4 with some success. RISM calculations reproduced experimental details in rough outline but, among other discrepancies, fell far short of experiment in predictions of the range over which pair correlation functions deviate from unity (randomness).

3. C_6H_6 vs. Spherical Molecules

Benzene clusters are particularly attractive subjects for investigation. They offer the possibility of studying in some detail a polyatomic, aspherical analogue of liquid clusters of nominally close-packed spheres. As will be seen, benzene behaves in some respects as quasispherical. So far, liquid clusters of rare gas atoms that might serve as reference examples have been seen only in computer simulations,[17,114,115] not experiment, perhaps because of their relatively narrow temperature range of stability and their resistance to supercooling. Whether an icosahedral motif appears in their liquid structure as has long been proposed, as well as in small solid clusters, has been answered definitively only very recently in molecular dynamics analyses of Stillinger.[116] In simulations of bulk liquids the structural patterns are so blurred by thermal motions that an objective assessment is difficult. Nevertheless, the local potential energy minimum in $3N - 6$ dimensional hyperspace describing the N-atom ensemble at a given moment *can* be determined and sampled at intervals. It is found that the geometric distribution of atoms corresponding to a characteristic potential energy minimum in hyperspace is independent of temperature, and that icosahedra make up only a minute fraction of the local groups in the bulk. Fragments with fcc packing can be joined to others in disordered aggregates more efficiently than can icosahedral fragments, evidently. Although the case against icosahedral packing in simple liquids looks compelling for bulk samples, it may very well be found that icosahedral packing will prevail in sufficiently small microdrops as it does in the microclusters they freeze to. Moreover, evidence suggesting that strong supercooling favors icosahedral units has been advanced.[117]

Unfortunately, conclusions available for benzene at the time of the present review are preliminary and incomplete. What can be said are the following. At ordinary pressures benzene freezes at 5.5 °C into orthorhombic crystals in which the molecular packing is often described as "herring bone" in pattern.[118] Nevertheless, if the disklike molecules are envisaged to puff up and undergo a smooth transformation to a spherical shape while maintaining the same packing arrangement, they reach the cubic closest packed (fcc) structure enjoyed by rare gas atoms. Moreover, also like rare gas atoms, their most stable packing in 13-molecule clusters is not the cuboctahedral fragment but is an icosahedron, according to calculations of packing energy.[91]

Under all expansion conditions leading to clusters so far explored with an initial vapor temperature of ~25 °C, the clusters have been observed to be liquidlike.[27,119] Typical structure functions are illustrated in Figure 2 for clusters produced with He, Ne, and Ar at a variety of mole fractions and pressures. Comparisons (Figure 6) with patterns calculated for 13-molecule clusters, cuboctahedral and icosahedral, and a 55-molecule crystal fragment show marked similarities but significant differences—differences related both to cluster size

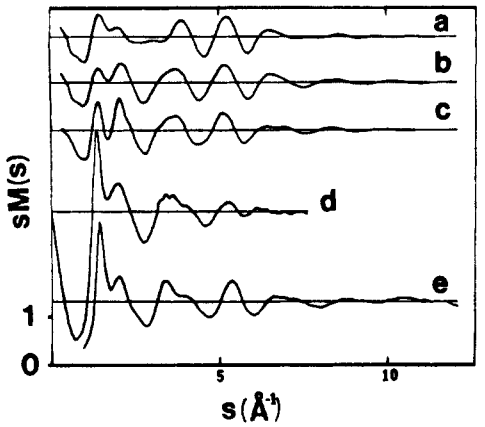

Figure 6. Structure functions for benzene. (a–c) Calculated, respectively, for Williams' 13 molecule cuboctahedral cluster and icosahedral cluster and for a 55 molecule, approximately spherical crystal fragment. (d) Narton's experimental X-ray intensities. (e) Electron diffraction intensities from clusters. Reproduced, with permission, from Valente.[27] Copyright 1984, American Institute of Physics, New York.

and packing. From the sharpness of the innermost ring it is estimated that the cluster diameter must be in excess of 32 Å; indeed, the ring is as sharp as that of bulk benzene. Preliminary evidence suggests that the supercooling may be substantial. Perhaps benzene's aspherical shape is responsible for a substantially higher activation energy for transition from supercooled liquid to crystal than is the case for monatomic clusters. No crystalline clusters have yet been seen although, when the most effective carrier, argon, was used under conditions designed to achieve high cooling, Ar clusters were formed as well as liquidlike benzene.

Simulations with RISM successfully represented the structure function *in the mean* (Figure 7) if atoms were inflated 6% over their true sizes according to the Williams potential functions. The detailed representation is not good, however, and is associated with a pair correlation function that is far more washed-out than that implied by experiment. Molecular dynamics and Monte Carlo simulations are widely believed to be superior to these or RISM for dense condensed phases. Although a number of investigators have carried out MD and MC computations on benzene[120–127] that reproduce the thermodynamic properties at room temperature reasonably well, they are of little use in interpreting the properties of cold clusters, quite apart from the disparity in temperature. Among other reasons, the potential functions they are based on are highly simplified and marginally realistic. Because of the considerable expense of MD and MC runs, only six-site models have been adopted, so far, instead of the 12-site model of Williams and Starr shown to give faithful representations of the crystal[123,124] for the high as well as the low pressure forms. In fact, the six-site models heretofore published have given rather crude crystal structures, whether they included the electrostatic quadrupole energy or not.

When computer simulations are refined to the point where they satisfactorily reproduce the diffraction patterns of clusters as well as giving a good account of thermodynamic properties, it can then be concluded that molecular interactions leading to clusters are fairly well understood. This degree of understanding has been at hand for monatomic substances for several years. It

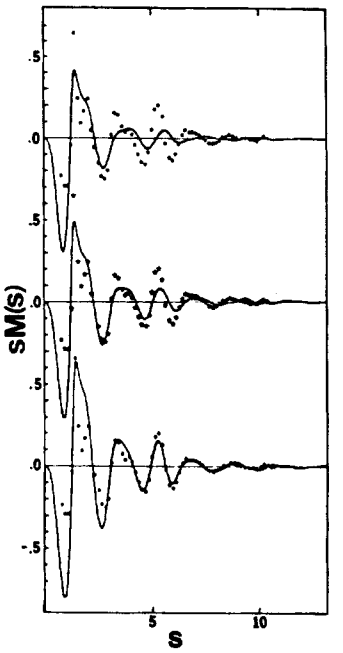

Figure 7. Structure functions for benzene. Points, electron diffraction intensities from clusters. Lines, RISM liquid simulations with various adjustments, curve (c) representing the best fit obtainable. For details see ref 27.

is only slowly being approached for liquidlike ensembles of polyatomic molecules.

4. *Other Liquidlike Clusters*

Too few systems have been investigated to establish general conclusions. As discussed in the foregoing section, monatomic, diatomic (in the single case examined), and very simple polyatomic molecules tend to form solid clusters. More complex polyatomic molecules apparently form liquid clusters easily. Examples so far seen include carbon tetrachloride and benzene (already discussed), cyclopropane, *n*-butane, neopentane, and perfluorobenzene.[109] Analyses of the latter examples are incomplete.

D. Trends in Nucleation and Cluster Growth

A comprehensive account of cluster formation in supersonic flow is far from having been achieved. On the one hand, it seems to be established that very small clusters are organized internally in a different way than are large clusters, and an underlying icosahedral packing is increasingly thought to characterize small assemblies of symmetrical molecules. On the other hand, small changes in the conditions of expansion have sometimes been seen to lead to substantial differences in molecular packing in clusters. In the case of the hexafluorides of sulfur, selenium, and tellurium three different crystalline forms have been produced,[24] and nucleation temperature more than cluster size seems to be the factor responsible. In the one example (CCl_4) so far seen to give both liquid and solid clusters, conditions favoring nucleation at a higher temperature were those giving the solid, and temperatures of the solid clusters appeared to be higher than those of the liquid, but not by a large margin.[26] It is possible under some conditions that disorganized clusters if formed at too low a temperature cannot transform quickly to the crystalline form. While this might account for the behavior of CCl_4, the modest differences in conditions

giving liquid and solid and the reasonably high cluster temperatures do not make for a convincing argument. The argument might, however, explain the fact that only liquid benzene clusters have been seen, so far.

It may be worthwhile to review briefly a few aspects of nozzle flow that afford some control over nucleation conditions. We will assume the nozzle is a Laval nozzle, a nozzle whose inner diameter increases smoothly with distance x from the throat. We will neglect effects of viscous drag in the boundary layer of gas close to the nozzle wall. Such effects are larger, the smaller the nozzle, but do not change greatly the behavior sketched below. To a good approximation the flow is adiabatic, attaining sonic velocity (Mach 1) at the point of greatest constriction, the throat. Therefore, the nozzle throughput is readily calculable[126] from the speed of sound

$$v_s = (\bar{\gamma}RT_1/\bar{M}_w)^{1/2} \tag{13}$$

and the throat area, A_0, where $\bar{\gamma}$ is the ratio $\bar{C}_p/\bar{C}_v$ of heat capacities of the gas mixture, $\bar{M}_w$ is the mean molecular weight, and T_1 is the temperature to which the gas falls when it has been accelerated to the speed of sound as discussed in the next paragraph. What accelerates the gas up to this point and beyond, of course, is the expansion of the gas upstream of it. The net increase in kinetic energy of flow of any volume element, on balance, is paid for by the enthalpy of that volume element. Therefore, gas with a high heat content by virtue of vibrational and rotational degrees of freedom can be accelerated to higher speeds in expansion than can a monatomic gas of comparable density whose heat capacity is solely translational. By the same token, a monatomic gas can undergo the greatest temperature drop in a given length of flow in the nozzle, and can cool a small amount of any gas seeded into it in like measure. This cooling is so great that even though the partial pressure p_s of the seeded gas decreases during expansion in the nozzle, the degree of supersaturation $p_s/p_s(\infty)$ rapidly increases, where $p_s(\infty)$ is the saturated vapor pressure of the bulk substance at the local temperature. When supersaturation reaches a critical level, nucleation of clusters becomes rapid. Then the heat of condensation evolved by the growing nuclei tends to raise the temperature of the flowing medium and shut off further nucleation.

To illustrate how the nucleation temperature and, thereby, cluster characteristics, can be controlled by varying flow conditions, we sketch a few more properties of flow in Laval nozzles. If $A(x)$ is the effective area of the nozzle at distance x from the nozzle throat, the temperature profile $T(x)$ is a simple function of $A(x)/A_0$ for a gas with a given γ ratio.[84] Since all rare gases have the same γ, their temperature profiles $T(x)$ are the same, and this is little changed by addition of a small mole fraction X_s of seeded vapor, as long as no heat of condensation has been given off. Moreover, $T(x)$ is independent of the initial pressure p_0. In addition, the well known relation between Mach number M (jet speed/speed of sound) and temperature expressing the conversion of enthalpy to mass flow rate, is

$$\frac{T_2}{T_1} = \frac{1 + ((\gamma - 1)/2)M_1^2}{1 + ((\gamma - 1)/2)M_2^2} \tag{14}$$

and is applicable to initial temperature ($M = 0$), throat temperature ($M = 1$) and flow temperature $T(x)$ at $M(x)$. Therefore $M(x)$, the profile of Mach number is the same for all monatomic carrier gases. What discriminates between the carrier gases is their molecular weights. Flow velocities and molecular speeds are both proportional to $(M_w)^{-1/2}$ according to eq 13 and 14. Helium will move over 3 times more quickly through a nozzle than will argon, but will contribute the same number of atom-cluster collisions (assuming the same pressure) because its atoms are over 3 times faster. Seeded molecules and clusters tend to be dragged along with the flow. Therefore, in a given distance Δx along the nozzle, seed–seed and seed–cluster collisions decrease in number the lighter is the carrier gas, because seed molecular speeds depend on $T(x)$ and seed M_w, not carrier M_w. Further enhancing the discrimination between carrier gases is the fact that energy exchange between atoms of carrier gas and surface molecules is more efficient if their masses are comparable. Therefore, argon atoms striking a cluster surface are, as a rule, far more efficient at extracting heat and cooling the cluster than are helium atoms. A final factor is mass fractionation, a phenomenon in which heavier particles tend toward the central flow lines while lighter particles move outward.[127] This effect is most pronounced with helium and has the effect of depleting the cooling power of the carrier gas in the region where the clusters are most concentrated.

Now let us consider how nucleation temperature can be controlled. If X_s, the seed mole fraction is small, the $T(x)$ profile is nearly that of the carrier and is independent of p_0, the total initial pressure. If X_s is fixed but p_0 is increased, or if p_0 fixed but X_s is increased, then a given degree of supersaturation will occur earlier in the nozzle and the nucleation temperature will be increased. To get nucleation at a lower temperature, initial conditions should be changed in the opposite direction. How mean cluster diameters D and the fraction f of seeded vapor that is condensed depend on flow conditions is exemplified by studies on benzene. Both experiment and computer simulations based on classical nucleation theory gave the following results:[27]

(1) At constant carrier stagnation pressure, reducing benzene mole fraction to small values causes D and f to decrease.

(2) At constant partial pressure of benzene, reducing carrier pressure causes D and f to decrease.

(3) As the molecular weight of carrier increases, D and f tend to increase.

(4) At saturated vapor pressure of benzene (20 °C), a carrier pressure of 2–3 bar is needed for a typical micronozzle (throat, 0.013 cm, exit 0.2 cm, length 3 cm, ref 24) to give reasonably complete condensation. These results can be understood after a little reflection in terms of the foregoing discussion. For further details, consult ref 27, 42, 43, 61, and 83.

V. Summary and Conclusions

Homogeneous nucleation in supersonic flow has proven to be a versatile technique for generating clusters. Mean cluster size can be controlled from a few molecules per cluster to over tens of thousands. Effects of cluster size on molecular packing have been documented in some detail for simple systems. Moreover, clusters of some substances can be induced to organize

in any of several different structural types, depending upon conditions of flow. Efforts to exploit this promising approach are at a very early stage.

Electron diffraction is one of the most effective experimental tools available for research on clusters. For crystalline clusters it can often determine in detail the molecular packing, cluster size, temperature, and density. For liquid and amorphous clusters the diffraction information is more limited. Computer simulations via Monte Carlo or molecular dynamics can provide supplementary evidence of considerable value for filling in details not resolved by the diffraction analyses. At the present state of the art, however, computer modeling is no more capable by itself than the diffraction analyses in deciphering details of disordered polyatomic systems because reliable, practical, potential surfaces are not yet generally avaialble. What appears to be a fruitful approach is to construct preliminary potential surfaces based upon available information about crystal structure, lattice dynamics, and thermodynamic information and to adjust, as needed, to fit the cluster data, in addition. In that way, by successive approximations, the internal structure, temperature, and density of even disordered clusters can be inferred. In the process of adjustment, realistic molecular interaction functions can be developed. This is presumably the ultimate goal in chemical research on clusters in the first place. Although most clusters studied by diffraction to date have been of highly volatile substances of marginal interest in, for example, reaction chemistry, high volatility is not an inherent requirement. If there were sufficient incentive, the technique could be extended to moderately refractory materials including various potential catalysts.

Because the approach described in the foregoing has been applied, so far, by only a handful of principal investigators, and because these investigators have been in widely different fields overlapping chemistry only modestly, the focus of this review has not been that of traditional chemistry. Yet it is clear that the type of information derivable is intrinsically of enormous importance in chemistry. It is to be hoped that the considerable potential of the method will be fully realized in the coming years.

VI. Acknowledgment

This work was supported by a grant from the National Science Foundation. I am indebted to Noel Kullavanijaya of Northwestern University for sending preprints of the late Professor G. D. Stein and for bringing various aspects of Professor Stein's research to my attention. A substantial fraction of the ideas and concepts sketched in this review derive from my colleagues J. Farges, B. Raoult, and G. Torchet at Orsay. The mistakes are mine, alone.

VII. References

(1) See, for example, Rymer, T. B. *Electron Diffraction*; Methuen: London, 1970. Vilkov, L. V.; Mastryukov, V. S.; Sadova, N. I. *Determination of the Geometric Structure of Free Molecules*; Mir: Moscow, 1983.
(2) Bonham, R. A.; Fink, M. *High Energy Electron Scattering*; Van Nostrand Reinhold: New York, 1974.
(3) Iijima, T., private communication, 1985.
(4) Hoare, M. R.; Pal, P. *Adv. Phys.* **1971**, *20*, 161.
(5) Hoare, M. R.; Pal, P. *Nat. Phys. Sci.* **1972**, *236*, 35.
(6) Hoare, M. R.; Pal, P. *J. Cryst. Growth* **1972**, *17*, 77.
(7) Hoare, M. R. *Adv. Chem. Phys.* **1979**, *40*, 49.
(8) Lee, J. K.; Barker, J. A.; Abraham, F. F. *J. Chem. Phys.* **1973**, *58*, 3166.
(9) Burton, J. *J. Catal. Rev. Sci. Eng.* **1974**, *9*, 209.
(10) Briant, C.; Burton, J. J. *J. Chem. Phys.* **1975**, *63*, 2045.
(11) Farges, J.; Raoult, B.; Torchet, G. *J. Chem. Phys.* **1973**, *59*, 3454.
(12) Farges, J.; de Feraudy, M. F.; Raoult, B.; Torchet, G. *J. Phys. (Les Ulis. Fr.)* **1977**, *C2*(7), 38.
(13) Farges, J. *Vide, Couches Minces* **1979**, *No.* 190, 22.
(14) Farges, J.; de Feraudy, M. F.; Raoult, B.; Torchet, G. *J. Phys. (Les Ulis, Fr.)* **1980**, *C3*(4), 41.
(15) Farges, J.; de Feraudy, M. F.; Raoult, B.; Torchet, G. *Acta Cryst.* **1982**, *A38*, 656.
(16) Farges, J.; de Feraudy, M. F.; Raoult, B.; Torchet, G. *Entre l'atome et le cristal: les agregats*; Cyrot-Lackmann, edite par, les editions de physique, Les Ulis, 1982; p 185.
(17) Farges, J.; de Feraudy, M. F.; Raoult, B.; Torchet, G. *J. Chem. Phys.* **1983**, *78*, 5067.
(18) Farges, J.; de Feraudy, M. F.; Raoult, B.; Torchet, G. *Ber. Bunsen-Ges. Phys. Chem.* **1984**, *88*, 211.
(19) Yokozeki, A.; Stein, G. D. *J. Appl. Phys.* **1978**, *49*, 2224.
(20) DeBoer, B. G.; Stein, G. D. *Surf. Sci.* **1981**, *106*, 84.
(21) Kim, S. S.; Stein, G. D. *Atmospheric Catalysis*; Mohnen, V. A., Schryer, D., Eds.; AGU: New York, 1982; 24 pages.
(22) Lee, J. W.; Stein, G. D. *Surf. Sci.* **1985**, *156*, 112.
(23) Lee, J. W.; Stein, G. D. *J. Chem. Phys.*, submitted for publication.
(24) Valente, E. J.; Bartell, L. S. *J. Chem. Phys.* **1983**, *79*, 2683.
(25) Bartell, L. S.; Valente, E. J.; Caillat, J., unpublished research.
(26) Valente, E. J.; Bartell, L. S. *J. Chem. Phys.* **1984**, *80*, 1458.
(27) Valente, E. J.; Bartell, L. S. *J. Chem. Phys.* **1984**, *80*, 1451.
(28) Mühlbach, J.; Sattler, K.; Pfan, P.; Recknagel, E. *Phys. Lett.* **1982**, *87A*, 415.
(29) Wegener, P. P.; Pouring, A. A. *Phys. Fluids* **1967**, *7*, 352.
(30) Pirenne, M. H. *The Diffraction of X-rays and Electrons by Free Molecules*; Cambridge University Press: London, 1946.
(31) Bonham, R. A.; Schafer, L. In *International Tables of Crystallography*; Ibers, J. A., Hamilton, W. C., Eds.; Kynoch: Birmingham, 1974; Vol. IV.
(32) Sellers, H. L.; Schafer, L.; Bonham, K. A. *J. Mol. Struct.* **1978**, *49*, 125.
(33) Tavard, C.; Nicolas, D.; Rouault, M. *J. Chim. Phys.* **1967**, *64*, 540.
(34) Heenan, R. K.; Bartell, L. S. *J. Chem. Phys.* **1983**, *78*, 1265.
(35) Bartell, L. S.; Heenan, R. K.; Nagashima, M. *J. Chem. Phys.* **1983**, *78*, 236.
(36) Torchet, G.; Bouchier, H.; Farges, J.; de Feraudy, M. F.; Raoult, B. *J. Chem. Phys.* **1984**, *81*, 2137.
(37) Yokozeki, A. *J. Chem. Phys.* **1978**, *68*, 3766.
(38) See, for example, Bartell, L. S. *J. Chem. Educ.* **1985**, *62*, 192.
(39) Bartell, L. S., unpublished research.
(40) Guinier, A. *X-ray Diffraction*; Freeman: San Francisco, 1963, p 121.
(41) DeBoer, B. G.; Kim, S. S.; Stein, G. D. *Rarefied Gas Dynamics*; Campargue, R., Ed.; Comissariat a L'Energie Atomique: Paris, 1979; p 1151.
(42) Sherman, P. M.; McBride, D. D.; Chmielewski, T.; Pierce, T. H.; Oktay, E. *Condensation of a Metal Vapor in a Supersonic Carrier Gas*; ARL Report 69-0089, Office of Aerospace Research, U.S. Air Force, 1969.
(43) Abraham, O.; Kim, S. S.; Stein, G. D. *J. Chem. Phys.* **1981**, *75*, 402.
(44) Wegener, P. P. In *Nonequilibrium Flows*; Wegener, P. P., Ed.; Marcel Dekker: New York, 1969.
(45) Bartell, L. S. "Electron Diffraction by Gases" In *Physical Methods of Chemistry*; Weissberger, A., Rossiter, B. W., Eds.; Wiley: New York, 1972; Vol. I, Part IIID.
(46) Soler, J. M.; Garcia, N.; Echt, O.; Sattler, K.; Recknagel, E. *Phys. Rev. Lett.* **1982**, *49*, 1857.
(47) Powers, D. E.; Hansen, S. G.; Geusic, M. E.; Puin, A. C.; Hopkins, J. B.; Dietz, T. G.; Duncan, M. A.; Longridge-Smith, P. R. R.; Smalley, R. E. *J. Phys. Chem.* **1982**, *86*, 2556.
(48) Elastic cross sections calculated via the optical theorem from the scattering factors of ref 32.
(49) Bonham, R. A.; Ng, E. W. *Chem. Phys. Lett.* **1969**, *4*, 355.
(50) Reid, R. C.; Prausnitz, J. M.; Sherwood, T. K. *The Properties of Gases and Liquids*, 3rd ed.; McGraw-Hill: New York, 1977.
(51) Bartell, L. S.; Jin, A. *J. Chem. Phys.* **1983**, *78*, 7159.
(52) Jin, A.; Bartell, L. S. *J. Chem. Phys.* **1983**, *78*, 7165.
(53) Kalman, E. *J. Appl. Crystallogr.* **1974**, *7*, 442; *Z. Phys. Chem. (Leipzig)* **1974**, *255*, 349.
(54) Bartell, L. S. *J. Chem. Phys.* **1975**, *63*, 3750.
(55) Miller, B. R.; Bartell, L. S. *J. Chem. Phys.* **1980**, *72*, 800.
(56) Bartell, L. S.; Raoult, B.; Torchet, G. *J. Chem. Phys.* **1977**, *66*, 5387.
(57) Raoult, B.; Farges. J. *Rev. Sci. Intrum.* **1973**, *44*, 430.
(58) Kim, S. S.; Stein, G. D. *Rev. Sci. Instrum.* **1982**, *53*, 838.
(59) Campargue, R. *Rev. Sci. Instrum.* **1963**, *35*, 111.

(60) Jeuck, P. R., 3rd; Saxon, G.; Stein, G. D. "Electron Diffraction Studies of Clustered Nozzle Beams". In *Rarefied Gas Dynamics*, Becker, M., Fiebig, M., Eds.; DFVLR: Porz-Wahn, Germany, 1974, F.9-1.
(61) Abraham, O.; Binn, J. A.; DeBoer, B. G.; Stein, G. D. *Phys. Fluids* **1981**, *24*, 1017.
(62) Hockney, R. W.; Eastwood, J. W. *Computer Simulations Using Particles*; McGraw-Hill: New York, 1981.
(63) Rahman, A. *Phys. Rev.* **1962**, *127*, 359.
(64) Temperley, H. N. V.; Trevena, D. M. "Liquids and their Properties"; Halsted: Chichester, 1978.
(65) Alder, B. J.; Hoover, W. G. In *Physics of Simple Liquids*; Temperly, H. N. V., Rowlinson, J. S., Rushbrooke, G. S., Eds.; North-Holland: Amsterdam, 1968.
(66) Jorgensen, W. L. *J. Am. Chem. Soc.* **1981**, *103*, 335, 341, 345.
(67) Pawley, G. S.; Thomas, G. W. *Phys. Rev. Lett.* **1982**, *48*, 410.
(68) See: Frish, H.; Lebowitz, J. L. *The Equilibrium Theory of Classical Fluids*; Benjamin: New York, 1964.
(69) See: McQuarrie, D. A. *Statistical Mechanics*; Harper and Row: New York, 1967; Chapter 13.
(70) Lowden, L. J.; Chandler, D. *J. Chem. Phys.* **1974**, *61*, 5228.
(71) Johnson, E.; Hazoumé, R. P. *J. Chem. Phys.* **1979**, *70*, 1599.
(72) Mackay, A. *Acta Cryst.* **1962**, *15*, 916.
(73) Farges, J.; de Feraudy, M. F.; Raoult, B.; Torchet, G. *Surf. Sci.* **1985**, *156*, 370.
(74) Farges, J.; de Feraudy, M. F.; Raoult, B.; Torchet, G. *Surf. Sci.* **1981**, *106*, 95.
(75) Kim, S. S.; Stein, G. D. *J. Colloid Interface Sci.* **1982**, *87*, 180.
(76) *Phys. Today*, **1985**, *38* (Feb.), 17.
(77) Nelson, D. R.; Halperin, B. I. *Science* **1985**, *229*, 233.
(78) Schechtman, D.; Blech, I.; Gratias, D.; Cahn, J. W. *Phys. Rev. Lett.* **1984**, *53*, 1951.
(79) Levine, D.; Steinhardt, P. *Phys. Rev. Lett.* **1984**, *53*, 2477.
(80) Kramer, P.; Neri, R. *Acta Cryst.* **1984**, *A40*, 580.
(81) Yamada, I.; Stein, G. D.; Usui, H.; Takagi, T. "Structure of Vaporized-Metal Clusters" to appear in Proceedings of the International Symposium on Ion Assisted Technology, 1982, six pages.
(82) This deviation, recognized in ref 37, was not, however, interpreted in terms of the structural model now accepted, but in terms of an erroneous identification of modulations of ring intensities with modulations of a liquid structure function. A liquid structure function would have given a continuous undulation as illustrated in Figure 2.
(83) Chmielewski, T.; Sherman, P. M. *AIAA J.* **1970**, *8*, 789.
(84) Crist, S.; Sherman, P. M.; Glass, D. R. *AIAA J.* **1966**, *4*, 68.
(85) In ref 27, constant B was given a smaller value that was supposed to apply to a *polyatomic* molecule on the basis of fragmentary information in ref 74. For clusters of *monoatomic* molecules the present value is better.
(86) Farges, J.; de Feraudy, M. F.; Raoult, B.; Torchet, G. "Rarefied Gas Dynamics", Part II; Potter, J. F., Ed.; *Progress in Atronautics and Aeronautics*, AIAA: New York, 1977; Vol. 51 p 1117.
(87) Farges, J.; de Feraudy, M. F.; Raoult, B.; Torchet, G. In *Rarefied Gas Dynamics*; Becker, M., Fiebig, M., Eds.; DFVLR: Porz-Wahn, 1974; Vol. II, F8-1.
(88) Farges, J. *J. Cryst. Growth* **1975**, *31*, 79.
(89) Audit, P. *J. Phys. (Paris)* **1969**, *30*, 192.
(90) Kim, S. S.; Shi, D. C.; Stein, G. D. *Rarefied Gas Dynamics*; Fisher, S. S., Ed.; AIAA: New York, 1981; p 1211.
(91) Van de Waal, B. W. *J. Chem. Phys.* **1983**, *79*, 3948.
(92) Torchet, G.; Schwartz, J. G.; de Feraudy, M. F.; Raoult, B. *J. Chem. Phys.* **1983**, *79*, 6196.
(93) Stein, G. D.; Armstrong, J. A. *J. Chem. Phys.* **1973**, *59*, 1999.
(94) Dowell, L. G.; Kohler, J. *Physica* **1934**, *1*, 655.
(95) Polk, D. E. *J. Non-Cryst. Solids* **1971**, *5*, 365.
(96) Steinhardt, P.; Alben, R.; Duffy, M. G.; Polk, D. E. *Phys. Rev.* **1973**, *B8*, 6021.
(97) Boutron, P.; Alben, R. *J. Chem. Phys.* **1975**, *62*, 4848.
(98) Kassner, J. L.; Hagen, D. E. *J. Chem. Phys.* **1976**, *64*, 1860.
(99) Stillinger, F. H.; Rahman, A. *J. Chem. Phys.* **1974**, *60*, 1545.
(100) Torchet, G.; Farges, J.; de Feraudy, M. F.; Raoult, B. *Rarefied Gas Dynamics*; Campargue, R., Ed.; CEA: Paris, 1979; Vol. II, p 1175.
(101) Wu, B. J. C.; Wegener, P. P.; Stein, G. D. *J. Chem. Phys.* **1978**, *68*, 308.
(102) Farges, J.; de Feraudy, M. F.; Raoult, B.; Torchet, G. Third International Symposium on Small Particles and Inorganic Clusters, Berlin, July 1984.
(103) Kim, S. S.; Stein, G. D. *J. Appl. Phys.* **1980**, *51*, 6419.
(104) Farges, J.; de Feraudy, M. F.; Raoult, B.; Torchet, G. *Surf. Sci.* **1985**, *156*, 444.
(105) Raynerd, G.; Tatlock, G. J.; Venables, J. A. *Acta Cryst.* **1982**, *B38*, 1896.
(106) Pawley, G. S.; Thomas, G., W. *Phys. Rev. Lett.* **1982**, *48*, 410. Pawley, G. S., private communication, 1985.
(107) Pawley, G. S.; Dore, M. T. *Chem. Phys. Lett.* **1983**, *99*, 45.
(108) Michel, J.; Drifford, M.; Rigny, P. *J. Chim. Physiochim. Biol.* **1970**, *67*, 31.
(109) Barshad, Y. Z.; Bartell, L. S., unpublished research.
(110) Angell, C. A.; Sare, J. M.; Sare, E. J. *J. Phys. Chem.* **1978**, *82*, 2622.
(111) Murata, Y.; Nishikawa, K. *Bull. Chem. Soc. Jpn.* **1978**, *51*, 411.
(112) Montague, D. G.; Chowdhury, M. R.; Dore, J. C.; Reed *J. Mol. Phys.* **1983**, *50*, 1.
(113) Chowdhury, M. R.; Dore, J. C. *J. Non-Cryst. Solids* **1981**, *46*, 343.
(114) Thompson, S. M.; Gubbins, K. E.; Walton, J. P. R. B.; Chantry, R. A. R.; Rowlinson, J. S. *J. Chem. Phys.* **1984**, *81*, 530.
(115) Powles, J. G.; Fowler, R. F.; Evans, W. A. B. *Chem. Phys. Lett.* **1983**, *96*, 289.
(116) Stillinger, F. H., private communication, 1985.
(117) Steinhardt, P. J.; Nelson, D. R.; Ronchetti, M. *Phys. Rev. Lett.* **1981**, *47*, 1287.
(118) Cox, E. G.; Cruickshank, D. W. J.; Smith, J. A. S. *Proc. R. Soc. London, A* **1958**, *247*, 1.
(119) Heenan, R. K.; Valente, E. J.; Bartell, L. S. *J. Chem. Phys.* **1983**, *78*, 243.
(120) Evans, D. J.; Watts, R. O. *Mol. Phys.* **1976**, *32*, 93.
(121) Claessens, M.; Ferrario, M.; Ryckaert, J.-P. *Mol. Phys.* **1983**, *50*, 217.
(122) Jorgensen, W. L.; Madura, J. D.; Swenson, C. J. *J. Am. Chem. Soc.* **1984**, *106*, 6638.
(123) Williams, D. E.; Starr, T. L. *Comput. Chem.* **1977**, *1*, 173.
(124) Dzyabchenko, A. V. *Zh. Strukt. Khim.* **1984**, *25*(3), 85; *Ibid.* **1984**, *25*(4), 57.
(125) Shi, X.; Sharkey, L.; Bartell, L. S., unpublished research, 1985.
(126) Kantrowitz, A.; Grey, J. *Rev. Sci. Instrum.* **1951**, *22*, 328.
(127) Anderson, J. B. In *Molecular Beams and Low Density Gasdynamics*; Wegener, P., Ed.; Dekker: New York, 1974.